THE JOURNAL OF PHYSICAL CHEMISTRY Letters

Letter

pubs.acs.org/JPCL

Role of the Dark $2A_g$ State in Donor−Acceptor Copolymers as a Pathway for Singlet Fission: A DMRG Study

Jiajun Ren,[†] Qian Peng,[‡] Xu Zhang,[†] Yuanping Yi,[‡] and Zhigang Shuai*[,†]

[†]MOE Key Laboratory of Organic OptoElectronics and Molecular Engineering, Department of Chemistry, Tsinghua University, Beijing 100084, People's Republic of China

[‡]Key Laboratory of Organic Solids, Beijing National Laboratory for Molecular Science (BNLMS), Institute of Chemistry, Chinese Academy of Sciences, Beijing 100190, People's Republic of China

Supporting Information

ABSTRACT: The mechanism of intramolecular singlet fission in donor−acceptor-type copolymers, especially the role of the dark $2A_g$ state, is not so clear. In this Letter, the electronic structure of the benzodithiophene (B)-thiophene-1,1-dioxide (TDO) copolymer is calculated by density matrix renormalization group theory with the Pariser−Parr−Pople model. We find that the dark $2A_g$ state is the lowest singlet excited state and is nearly degenerate with the $1B_u$ state. So, a fast internal conversion from $1B_u$ to $2A_g$ state is highly possible. The $2A_g$ state has a strong triplet pair character, localized on two neighboring acceptor units, which indicates that it is an intermediate state for the intramolecular singlet fission process. With the increase of the donor−acceptor push−pull strength in our model, this triplet pair character of the $2A_g$ state becomes more prominent, and meanwhile the binding energy of this coupled triplet pair state decreases, which favors the separation into two uncoupled triplet states. We propose a model in which the competition between the singlet fission process and the nonradiative decay process from the $2A_g$ state would determine the final quantum yield.

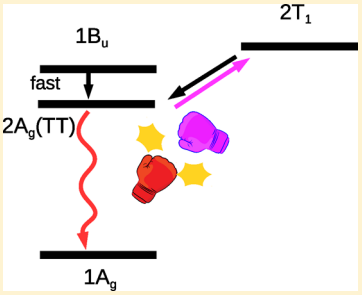

Singlet fission (SF) phenomenon is very useful for photovoltaic devices, due to its potential to break the Shockley−Queisser theoretical limit to the efficiency of a single junction solar cell.[1,2] Typical intermolecular SF (xSF) systems, such as tetracene and pentacene, have been widely investigated both in experimental and theoretical studies, as summarized in recent reviews.[3,4] However, no efficient intramolecular SF (iSF) system has been found until recently.[5−8] The iSF system is much more attractive, because its SF efficiency is not sensitive to intermolecular packing, which is difficult to control in the processing technics. Among the iSF systems, the majority are covalently linked tetracene and pentacene hetero- or homo-dimers.,[6−8] extending directly from the former xSF systems. Another iSF system, the donor−acceptor (DA)-type conjugated copolymer, benzodithiophene (B)-thiophene-1,1-dioxide (TDO), was first found to have a very high iSF efficiency (~170%).[5] Considering the abundant family of DA copolymer, it is highly possible to discover and design more efficient iSF systems. Nonetheless, only one DA copolymer with a high iSF efficiency has been reported so far, and the iSF mechanism is still not so clear.[5,9−11]

In the singlet fission process, according to Kasha's rule, the most important state is a low lying singlet state with a prominent double excitation character, composed of two coupled triplet states. Thus, it is usually called triplet pair state (^{1}TT) or multiexciton state (ME), which is able to split into two independent triplets. Some quantum chemistry calculations indeed revealed that a low adiabatic state with a ^{1}TT character exists in the noncovalent dimers[12−15] and covalently linked dimers.[16,17] In the former studies of some homopolymers like polyene, the lowest singlet excited state with A_g symmetry has been described as a ^{1}TT state.[18,19] Recent theoretical studies on iSF in a small molecule, quinoidal bithiophene, also showed that the lowest $2A_g$ singlet excited state is a ^{1}TT state.[20,21] To explain the iSF in the DA copolymers, Mazumdar et al. proposed a mechanism that the broken symmetry would mix charge transfer (CT) state into the $2A_g(^1TT)$ state, which makes the original $2A_g(^1TT)$ dark state in the homopolymer optically allowed. So the ^{1}TT state could directly absorb light and split into two triplet states.[22] On the contrary, Busby et al. suggested that in the PBTDOn system, the $2A_g$ state is an excited state nonradiative decay pathway, in competition with iSF directly from the $1B_u$ state.[5,23] The different points of view toward the $2A_g$ state prevent further understanding the whole photophysical processes in this system.

Our intention is to address the question of what the role of the $2A_g$ state is in the iSF process in the DA copolymer and how the donor−acceptor electronic push−pull strength affects this process. Since the electronic structure, especially the correct energy level order, is fairly essential, and the ^{1}TT state is mainly a double excitation state, high level electronic structure theory is a necessity. It was demonstrated that even the equation-of-motion coupled cluster single and double method

Received: March 19, 2017
Accepted: May 1, 2017
Published: May 1, 2017

DOI: 10.1021/acs.jpclett.7b00656
J. Phys. Chem. Lett. 2017, 8, 2175−2181

(EOM-CCSD) produced the wrong order for polyenes longer than 20 π-electrons.[24] Density matrix renormalization group theory (DMRG)[25] has been widely adopted as a powerful wave function ansatz to treat static correlation dominant systems in quantum chemistry, especially in one- and quasi-one-dimensional systems.[26,27] Our recent development also extends the application of DMRG.[28] Herein, we use a symmetrized DMRG method[29] to calculate the electronic structure of a few lowest adiabatic states of PBTDO1 oligomer with the Pariser−Parr−Pople (PPP) model[30,31] (see eq 1).

$$\hat{H}_{\mathrm{PPP}} = \sum_{i\sigma} \varepsilon_i \hat{a}_{i\sigma}^{\dagger}\hat{a}_{i\sigma} + \sum_{\{ij\}\sigma} t_{ij}\hat{a}_{i\sigma}^{\dagger}\hat{a}_{j\sigma} + \sum_{i} U_i \hat{n}_{i\uparrow}\hat{n}_{i\downarrow} + \sum_{i<j} V_{ij}(\hat{n}_i - Z_i)(\hat{n}_j - Z_j) \quad (1)$$

Here, the first term and the second term represent the site energy and nearest neighbor hopping, respectively. The third term is the Hubbard term representing the on-site Coulomb repulsion, and the last term represents the long-range Coulomb interaction.

The chemical structure of PBTDO1 is shown in Figure 1a. ADADADA oligomer (n = 3) is chosen as our model system to mimic the polymer. The structure is first optimized at the b3lyp/6-31g(d) level by the Gaussian 09 package[32] under the restriction of the C_{2h} point group symmetry. Then the conjugated backbone (the red part in Figure 1a) is selected to construct the PPP model Hamiltonian. The sulfer atom in thiophene dioxide is neglected because the p orbitals are all saturated by bonding with two oxygen atoms. Therefore, the thiophene-dioxide is simplified to cis-butadiene in the PPP model. This simplification is reasonable, in that the photophysical property of poly thiophene-dioxide is more like polyene rather than polythiophene.[33] The site energy difference $\varepsilon_{\mathrm{DA}}$ between the donor and acceptor units is used to represent the electronic push−pull strength (see 1b), which we call DA strength. ε_1 and ε_2 respectively represent the site energy difference due to the electron inductive effect of the methoxyl group and sulfur dioxide group. The parameters are fetched from the ZINDO package[34] or fitted carefully. The details are provided in the Supporting Information (SI) Section 1. The optimal parameters are ε_1 = 1.0 eV, ε_2 = −0.7 eV, and $\varepsilon_{\mathrm{DA}}$ = 1.5 eV. In addition, the accuracy of the DMRG method depends on the number of retained many-body basis states (M). After benchmarking, we choose M = 1024 in all the calculations, which is already accurate enough in our problem (see Table S2).

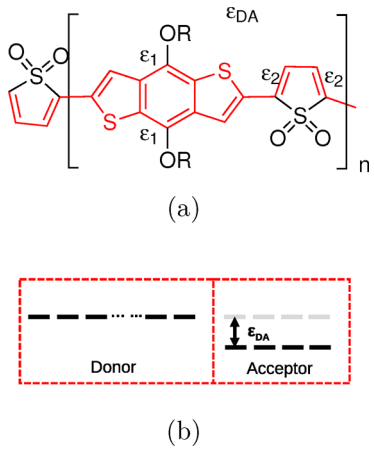

Figure 1. (a) The chemical structure of PBTDO1, where the conjugated backbone is shown in red. The n = 3 oligomer with C_{2h} symmetry is calculated in this Letter. (b) The site energy difference $\varepsilon_{\mathrm{DA}}$ between the donor and acceptor atomic orbitals to represent the DA push−pull strength.

To study the effects of the electronic push−pull strength between the donor and acceptor on the electronic structure, the DA strength $\varepsilon_{\mathrm{DA}}$ varies from 1.5 to 5.5 eV. In this range, the relative energy level alignment of D and A is not changed (see Figure S1). The frontier orbitals of PBTDO1/ADADADA oligomer are shown in Figure S2, which is almost the same as what we get from ab initio calculation. In Figure 2, we plot the excitation energies of the lowest three excited states, $1B_u$, $2A_g$, and twice T_1 of PBTDO1/ADADADA oligomer as a function of the DA strength $\varepsilon_{\mathrm{DA}}$. The excitation energy of the $1B_u$ state at $\varepsilon_{\mathrm{DA}}$ = 1.5 eV is 1 eV larger than the optical gap measured in the experiments.[5] This is due to the model Hamiltonian, in which only the minimum p_z atomic orbitals are considered and then most dynamic correlation is neglected. However, the trend with the DA strengths is still worth analyzing. The excitation energies would monotonically decrease when the DA strength increases. Meanwhile, the energies of the $1B_u$ and $2A_g$ state are nearly degenerate (~20 meV) when $\varepsilon_{\mathrm{DA}}$ is less than 3.5 eV, indicating that a very fast internal conversion would happen from the $1B_u$ state to the $2A_g$ state. In addition, we use the "Natural Transition Orbital" (NTO) method[35] to preliminarily identify the character of the $2A_g$ and $1B_u$ states. In the configuration interaction singles method (CIS) and the time-dependent density functional theory (TDDFT), the sum of the square of each NTO pair singular value $\sum_s \Gamma_s^2$ is exactly 1 (also the square of the norm of the virtual-occupied block of one-particle reduced transition density matrix). The magnitude of each singular value represents the proportion of such NTO pair in the excited state. However, if the excited state is not a pure single excitation state (like the DMRG many body wavefunciton), $\sum_s \Gamma_s^2$ would not be 1. All of these arguments are based on the assumption that the ground state is a Hartree−Fock configuration. This assumption is reasonable, since the ground state is weakly correlated in most closed-shell organic molecules and the Hartree−Fock configuration is the leading

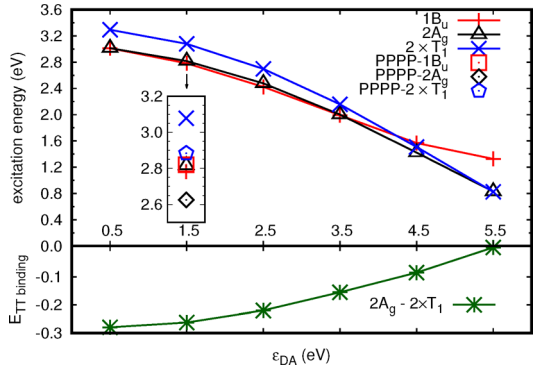

Figure 2. Excitation energies of the $1B_u$, $2A_g$ and twice T_1 states of PBTDO1/ADADADA oligomer as a function of DA strength. The inset figure also plots the energy after PPP-Peierls optimization on the $2A_g$ state at $\varepsilon_{\mathrm{DA}}$ = 1.5 eV. The triplet pair binding energy $E_b = E_{2A_g} - 2 \times E_{T_1}$ is shown in green.

DOI: 10.1021/acs.jpclett.7b00656
J. Phys. Chem. Lett. 2017, 8, 2175−2181

term. So, $\sum_s \Gamma_s^2$ would be smaller than 1 and represent the proportion of single excitation components in the excited state.

We list the largest three Γ_s^2 and $\sum_s \Gamma_s^2$ of $1A_g-2A_g$ and $1A_g-1B_u$ states in Table 1. The $2A_g$ and $1B_u$ states have totally

Table 1. Largest Three and the Total Sum of the NTO Singular Values Γ_s^2 of the $1A_g-2A_g$ and $1A_g-1B_u$ States

	ε_{DA}/eV	0.5	1.5	2.5	3.5	4.5	5.5
$2A_g$	1	0.107	0.127	0.136	0.111	0.073	0.051
	2	0.074	0.069	0.060	0.050	0.044	0.041
	3	0.025	0.024	0.017	0.008	0.004	0.003
	total	0.233	0.242	0.229	0.179	0.126	0.099
$1B_u$	1	0.491	0.497	0.500	0.493	0.465	0.435
	2	0.178	0.169	0.156	0.136	0.108	0.057
	3	0.062	0.049	0.038	0.033	0.028	0.008
	total	0.793	0.766	0.739	0.701	0.632	0.514

different excitation character. When ε_{DA} = 1.5 eV, the $\sum_s \Gamma_s^2$ of the $1B_u$ state is 0.766, and the $\sum_s \Gamma_s^2$ of the $2A_g$ state is 0.242. Therefore, the $1B_u$ state is mainly a single excitation state, whose main character is an electronic charge transfer from the donor to the acceptor, according to the first two NTO pair orbitals shown in Figure S3. By contrast, the $2A_g$ state is mainly a double excitation state, which is identified below as a ^{1}TT state. The binding energy E_b of the triplet pair state is the energy difference between the adiabatic coupled ^{1}TT state and two independent T_1 states, which is a result of the configuration interaction between the pure ^{1}TT state and the other singlet states.[16,36] Hence, E_b is considered as the minimum energy to be overcome for the coupled ^{1}TT state to separate. $E_b = E_{2A_g} - 2 \times E_{T_1}$ is plotted in Figure 2 (shown in green), which is negative and decreases (absolute value) when DA strength increases. From the thermodynamics point of view, smaller ^{1}TT binding energy is better for the ^{1}TT state to separate. So larger DA strength favors the separation. The excitation energies and ^{1}TT binding energies of the BTDO1/ADA molecule and the BTDO2/AADAA molecule are also plotted in Figure S4, sharing the same feature as PBTDO1/ADADADA. We also use the PPP-Peierls model[37] to optimize the molecular structure of PBTDO1/ADADADA at the $2A_g$ state when ε_{DA} = 1.5 eV. The electrons and lattice are coupled together by the effects of changes in the bond length on the one-electron hopping integral. The PPP-Peierls model Hamiltonian is as follows:

$$\hat{H}_{PPPP} = \hat{H}_{PPP} + \sum_{\{ij\},i>j,\sigma} \alpha\Delta_{\{ij\}}(a_{i\sigma}^{\dagger}a_{j\sigma} + a_{j\sigma}^{\dagger}a_{i\sigma}) + \frac{1}{2}\sum_{\{ij\},i>j} K_{\{ij\}}\Delta_{\{ij\}}^2 \quad (2)$$

Here, $\Delta_{\{ij\}}$ denotes the change of bond length u_j-u_i. u_i is the displacement of atom i. α denotes the linear electron−phonon coupling parameter. $K_{\{ij\}}$ is the spring constant of each bond. The same parameters are adopted from polyene calculation, α = 4.593 eV Å^{-1}, $K_{\{ij\}}$ = 46 eV Å^{-2}.[38] The excitation energies of the $2A_g$ state and the T_1 state decrease a lot, while the excitation energy of the $1B_u$ state increases a little bit (see Figure 2). The similar electron−phonon coupling effect on the $2A_g$ and T_1 states implies some similarity in the electronic structure of them. We will analyze the structure of the $2A_g$ state wave function in detail with four different wave function analysis methods: (i) local spin analysis; (ii) real space double-spin flip density analysis; (iii) spin−spin correlation function analysis; (iv) bond order analysis.

In many other theoretical studies, they use the percentage of double excitation configurations[15,22] or analyze the dominant configuration based on local orbitals[13,14,39] to determine whether the excited state is a ^{1}TT state. On one hand, it is difficult to define local orbitals physically in this polymer system, as we could do in the dimer system. On the other hand, acquiring the coefficient of each configuration from the DMRG wave function is knotty. So, we borrow the concept of "local spin"[40] to identify the ^{1}TT state, since each triplet component occupies a different position in the real space. Though it is not a real physical quantity that can be measured in the experiments, local spin analysis is very helpful to analyze the contribution from a fragment to the total spin $\langle\hat{S}^2\rangle$.

$$\langle\hat{S}^2\rangle = \sum_A \langle\hat{S}_A^2\rangle + \sum_{A,B,A\neq B} \langle\hat{S}_A\hat{S}_B\rangle \quad (3)$$

The operator $\hat{S}_A$ is obtained by multiplying the total spin operator $\hat{S}$ with an appropriate atomic projector. When dealing with the SF problem, local spin was first introduced by Krylov et al. to identify the ^{1}TT state in the molecular dimer.[41] In the simple 4 electrons 4 orbitals xSF dimer model, the local spin $\langle\hat{S}_{A/B}^2\rangle$ of molecule A or B calculated from the purely constructed spin-adapted $|T_AT_B\rangle$ wave function is exactly 2, which means it is completely a coupled triplet pair state. We calculate the local spin of half the ADADADA oligomer in the $1A_g$, $2A_g$, and $1B_u$ states with the DMRG wave function (see Figure 3). The calculation details are presented in SI section 4.

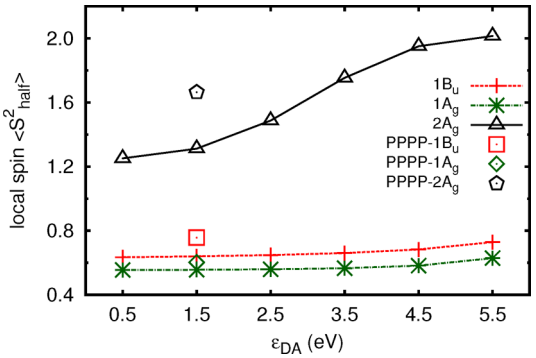

Figure 3. Local spin of half the PBTDO1/ADADADA oligomer (fragment from site 1 to 26 shown in Figure 4d) in the $1A_g$, $2A_g$, and $1B_u$ states as a function of DA strength ε_{DA}.

At different DA strengths ε_{DA}, the local spin $\langle\hat{S}_{half}^2\rangle$ of the $2A_g$ state is always over 1.2, while that of $1A_g$ and $1B_u$ states are always near 0.6. With the increase of ε_{DA}, $\langle\hat{S}_{half}^2\rangle$ of the $2A_g$ state is approaching 2.0, indicating that the $2A_g$ state is constructed by two pure triplet states. In other words, large DA strengths increase the percentage of TT configuration in the $2A_g$ wave function. Furthermore, after relaxing the structure on the $2A_g$ state with the PPP-Peierls model at ε_{DA} = 1.5 eV, the local spin $\langle\hat{S}_{half}^2\rangle$ of the $2A_g$ state increases from 1.31 to 1.66, indicating that the optimized structure of the $2A_g$ state would stabilize the ^{1}TT component, while the other two states show no clear increase. The local spin of BTDO1/ADA and BTDO2/AADAA molecules are also calculated, and they behave in a similar manner (see Figure S5). Therefore, we identify that the $2A_g$ state has a dominant ^{1}TT configuration, which becomes more prominent when DA strength increases or after the

DOI: 10.1021/acs.jpclett.7b00656
J. Phys. Chem. Lett. 2017, 8, 2175−2181

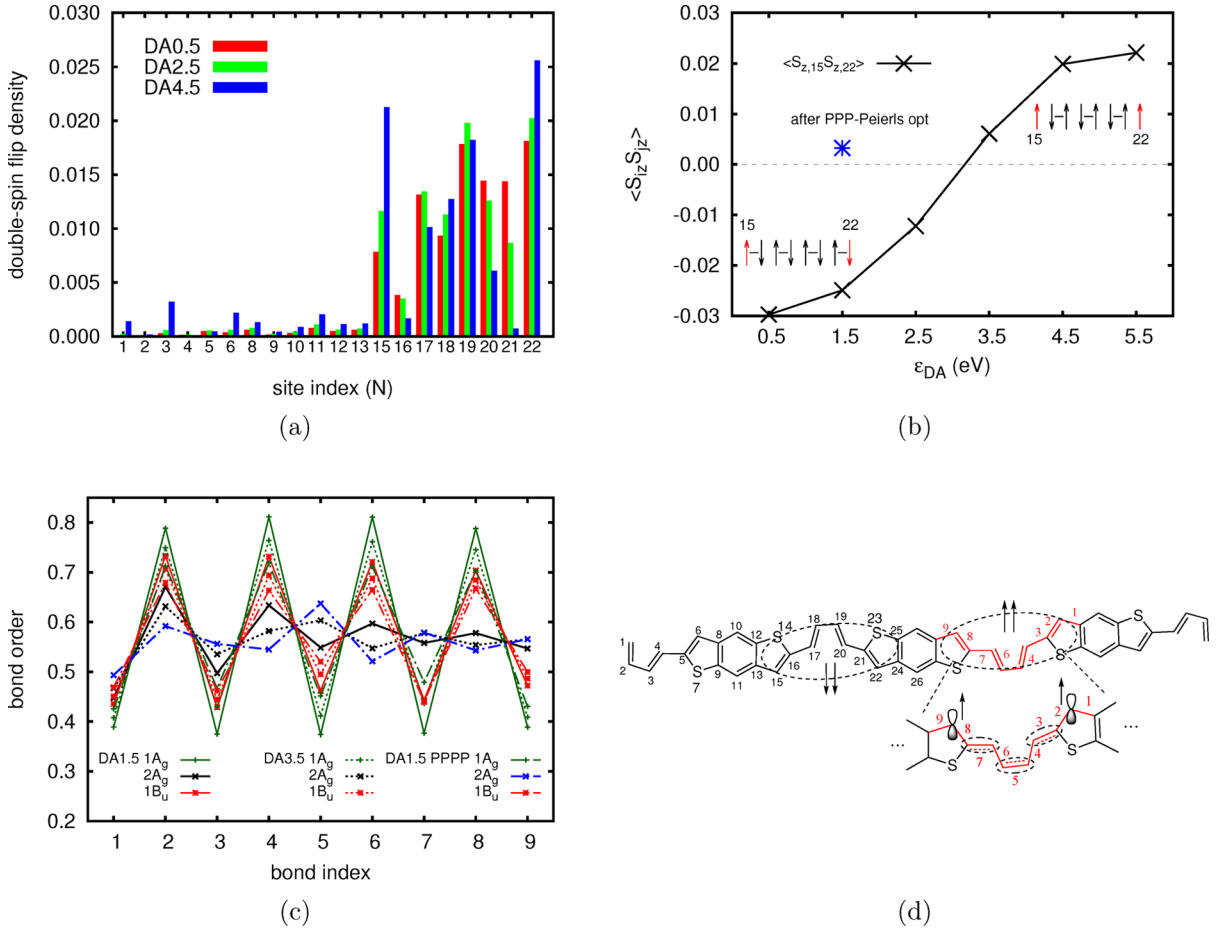

Figure 4. (a) Real space double-spin flip density between the $1A_g$ state and the $2A_g$ state of PBTDO1/ADADADA oligomer. (b) The spin−spin correlation function pattern between sites 15 and 22 at different DA strengths. The schematic spin diagram is included. (c) The bond order of the $1A_g$, $2A_g$,and $1B_u$ states of PBTDO1/ADADADA oligomer when ε_{DA} = 1.5 eV and ε_{DA} = 3.5 eV. (d) Schematic representation of ^{1}TT structure of the $2A_g$ state in PBTDO1/ADADADA oligomer.

structure relaxes on the $2A_g$ state. By contrast, the other singlet states only have a small ^{1}TT component. That is why the effect of electron−phonon coupling in the $2A_g$ state and the T_1 state is very similar above.

Real space double-spin flip density patterns are used to characterize the bimagnon character.[42] In this system, the $2A_g$ state has a triplet−triplet bimagnon character. The double-spin flip density flips an electron spin from σ to $-\sigma$ on an orbital at $R - r/2$ and simultaneously flips an electron spin from $-\sigma$ to σ on an orbital at $R + r/2$, where R is set at the center of a polymer chain and r is the triplet pair separation length. The expression in the formalism of second quantization is as follows, which is obtained by a two-particle reduced transition density matrix.

$$\langle \psi_{ES} | c^{\dagger}_{p,\sigma} c_{p,-\sigma} c^{\dagger}_{n-p,-\sigma} c_{n-p,\sigma} | \psi_{GS} \rangle \tag{4}$$

Here, $\sigma = \{\uparrow,\downarrow\}$, p is the index of the C p_z orbital, and n is the total number of p_z orbitals in the chain. ES denotes excited state and GS denotes ground state. The double-spin flip transition density between $|\psi_{2A_g}\rangle$ and $|\psi_{1A_g}\rangle$ is plotted in Figure 4a. Since the system has C_{2h} symmetry, only half of the system is shown. The ^{1}TT state is mainly localized on two neighboring acceptor units. The fragment from atom 15 to atom 22 (from bond 1 to 9 in red) shown in Figure 4d, which is similar as a short polyene fragment, is the most important structure for each triplet state. Moreover, with the increase of DA strength, the density increases and extends, indicating that each triplet component is enhanced and becomes more extended.

The spin−spin correlation function $\langle \hat{S}_{iz} \hat{S}_{jz} \rangle$ is used to show the correlation of spin alignment in the real space.[38] If one site has one electron, electrons can hop to decrease the total energy only when the spins of the neighboring sites are antiparallel. Consequently, in the ground state, the spins tend to be oriented antiparallel between neighboring sites, and the spin−spin correlation function is alternated with positive and negative in a conjugated chain. While in the $2A_g$ state, the spin−spin correlation function pattern is different. Take the spin−spin correlation $\langle \hat{S}_{15,z} \hat{S}_{22,z} \rangle$ between site 15 and site 22 as an example (see Figure 4b). It obeys the antiparallel rule like the ground state when ε_{DA} is small. By contrast, with the increase of ε_{DA}, $\langle \hat{S}_{15,z} \hat{S}_{22,z} \rangle$ approaches 0, revealing that the $|\uparrow\uparrow\rangle$ and $|\uparrow\downarrow\rangle$ configuration on sites 15 and site 22 has almost the same weight. As the ε_{DA} further increases, $\langle \hat{S}_{15,z} \hat{S}_{22,z} \rangle$ becomes positive, which means that the electrons on sites 15 and site 22 are spin parallel, indicating a triplet configuration. After PPP-Peierls optimization on the $2A_g$ state when ε_{DA} = 1.5 eV, the $\langle \hat{S}_{15,z} \hat{S}_{22,z} \rangle$ turns from negative to positive, showing an enhanced triplet character, which is consistent with the local spin analysis above.

We plot the bond order $\langle \psi | \sum_{\sigma} a^{\dagger}_{i\sigma} a_{j\sigma} + a^{\dagger}_{j\sigma} a_{i\sigma} | \psi \rangle$ of the $1A_g$, $2A_g$, and $1B_u$ states for bond indices 1 to 9 in Figure 4c. The

DOI: 10.1021/acs.jpclett.7b00656
J. Phys. Chem. Lett. 2017, 8, 2175−2181

bond order of $1A_g$ and $1B_u$ states has a normal single bond−double bond alternation. However, in the $2A_g$ state, near the center donor unit, this alternation is averaging. It is characteristic that the component of quinoid resonance structure becomes large. After relaxing the structure on the $2A_g$ state with the PPP-Peierls model, the single bond−double bond alternation of the $2A_g$ state would even be reversed. This indicates that the quinoid resonance structure is more favorable in the $2A_g$ state. This averaging or even reverse of the single bond−double bond alternation character is a result of local triplet state, similar to the case of polyene,[18] where the unpaired electrons weaken the bonding interaction (see Figure 4d).

From the above analysis, we discover that the $2A_g$ state has a large ^{1}TT component, consistent with some former studies of polymers and small molecules.[18−21] Additonally, the ^{1}TT state is localized on two neighboring acceptor units. That is why the small molecule BTDO1, with merely a minimum ADA structure, also has the iSF phenomenon. Therefore, the $2A_g$ state is the only one low lying excited state that is possible to play the role of the ^{1}TT intermediate state triggering the singlet fission process. Based on our calculations, we propose a model to explain the mechanism of iSF in such a polymer (see Figure 5a). Since the $1B_u$ and $2A_g$ states are nearly degenerate, the internal conversion process from $1B_u$ to $2A_g$ state (SF step I) is very fast. And then, the $2A_g$ state, with a large ^{1}TT component, would split into two uncoupled triplets (SF step II). Meanwhile, two independent triplets would recombine to the $2A_g$ state through the triplet−triplet annihilation (TTA). The $2A_g$ state would also decay to the ground state through the nonradiative process. This model for iSF in the polymer is almost the same as what was proposed by Kolomeisky and Krylov et al.[16,36] for xSF in the molecular crystals and iSF in the covalently linked dimers. The only difference is that the SF step I is very fast because of the near degeneracy of the $1B_u$ and $2A_g$ states. Under this condition, only the SF step II and the competitive nonradiative decay from the $2A_g$ state to the ground state should be considered.

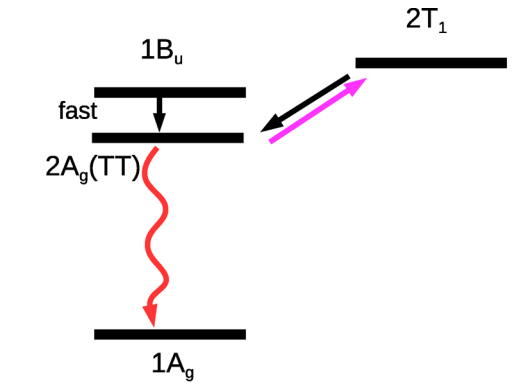

(a)

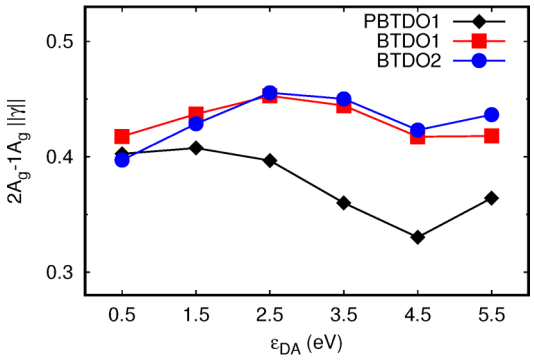

(b)

Figure 5. (a) Diagram of the singlet fission process in the PBTDO1 system. (b) Norm of symmetric one-particle reduced transition density matrix between the $1A_g$ and $2A_g$ states.

To calculate the nonradiative decay rate, the nonadiabatic coupling (NAC) between the $2A_g$ and the $1A_g$ states needs to be calculated, which is difficult with DMRG theory or any other high level electronic structure theory. Since the NAC is a one-electron operator, Krylov et al. proposed to use the norm of one-particle reduced transition density matrix to approximate the NAC.[14,41] Based on the Cauchy−Schwarz inequality,

$$\gamma_{pq}^{if} = \langle \psi_i | p^\dagger q | \psi_f \rangle \tag{5}$$

$$\langle \psi_i | \hat{A} | \psi_f \rangle = \mathrm{Tr}[\gamma^{if} A] \le \left\| \gamma \right\| \cdot \left\| A \right\| \tag{6}$$

Herein,

$$\| \gamma \|^2 = \mathrm{Tr}[\gamma \gamma^\dagger] = \sum_{pq} \gamma_{pq} \gamma_{qp} \tag{7}$$

These two quantity A_{if} and $\|\gamma\|$ are well correlated in most cases in the former studies.[41] In addition, because only the symmetric part of γ ($\gamma^s = \frac{1}{2}(\gamma + \gamma^T)$) contributes to the properties associated with real-valued Hermitian operators and real-valued wave functions,[41] we use $\|\gamma^s\|$ to estimate the trends in NAC. $\|\gamma^s\|_{1A_g-2A_g}$ of PBTDO1/ADADADA, BTDO1/ADA, and BTDO2/AADAA are calculated at different DA strengths ε_{DA} (see Figure 5b). The small molecules BTDO1 and BTDO2 have a similar $\|\gamma\|$, while the oligomer PBTDO1/ADADADA has a smaller $\|\gamma\|$ in the whole range of ε_{DA}, indicating that PBTDO1 has a smaller NAC between the $2A_g$ and the $1A_g$ states. On the other hand, in the experimental measurement, the optical bandgaps of PBTDO1, BTDO1, and BTDO2 are respectively 1.79, 1.85, 1.65 eV.[5] Since the $1B_u$ state is the bright state and is nearly degenerate with the dark $2A_g$ state in our calculation, we approximate that the energy of $2A_g$ states in these three systems is roughly the same as the optical gap. According to the energy gap law,[43] a larger energy gap indicates a smaller Franck−Condon factor. So, the Franck−Condon factor of the nonradiative transition from the $2A_g$ state to the $1A_g$ state in PBTDO1 is smaller than that in BTDO2. Based on the Fermi−Golden rule,

$$k_{nr} \sim \mathrm{NAC}^2 \cdot \mathrm{FC}^2 \tag{8}$$

the nonradiative decay rate of PBTDO1 is smaller than that of BTDO1 and BTDO2. Therefore, although all these three similar systems have a ^{1}TT configuration dominant $2A_g$ state from our above calculations, the nonradiative decay rate would be more competitive than the singlet fission rate in BTDO1 and BTDO2, which could qualitatively explain the observation that only PBTDO1 has a high singlet fission yield in the experiments.[5] To demonstrate the rationality of the model in Figure 5a, we also adopt some empirical parameters and solve it numerically to see the real-time state population. The details

DOI: 10.1021/acs.jpclett.7b00656
J. Phys. Chem. Lett. 2017, 8, 2175−2181

are provided in SI section 6. When $k_{SF} > k_{nr}$($k_{SF} < k_{nr}$), the quantum yield of the triplet states is high(low), and the lifetime is long(short), which qualitatively accords well with the bleach recovery in transient absorption measurements of PBTDO1 and BTDO1, respectively[5] (see Figure S8).

In summary, we use the DMRG method to investigate the electronic structure of the new singlet fission system, DA-type copolymer PBTDO1. We also try to answer a puzzle in the existing studies whether the dark $2A_g$ state in the DA copolymer is a singlet fission pathway or a nonradiative decay pathway. First, we find that the $2A_g$ state is the lowest excited state in such system, nearly degenerate with the bright $1B_u$ state. Through four different wave function analysis methods, we identify that the $2A_g$ state of PBTDO1 has a prominent ^{1}TT character, which is localized on two neighboring acceptor units. Thus, the ADA structure is the minimum requirement to design this kind of iSF system. Moreover, large DA push−pull strength would increase the ^{1}TT component in the $2A_g$ state and decrease the ^{1}TT binding energy, which is good for the separation into two independent triplets. So, the strong donor and strong acceptor units are preferred for the molecular design. Therefore, the $2A_g$ state is essential for the iSF process. We propose that the system would undergo a fast $1B_u$ state to $2A_g$ state internal conversion, and then the $2A_g$ state could split into two triplets. However, the nonradiative decay from the $2A_g$ state to the ground state would compete with the iSF process, which would lead to different behaviors in the small molecules BTDO1 and BTDO2.

■ ASSOCIATED CONTENT

Supporting Information

The Supporting Information is available free of charge on the ACS Publications website at DOI: 10.1021/acs.jpclett.7b00656.

Parameter fitting procedure, derivation of local spin in the PPP model, numerical solution of the kinetic model, and the excitation energies and local spin analysis of BTDO1/ADA and BTDO2/AADAA molecules (PDF)

■ AUTHOR INFORMATION

Corresponding Author

*E-mail: zgshuai@tsinghua.edu.cn.

ORCID

Jiajun Ren: 0000-0002-1508-4943
Qian Peng: 0000-0001-8975-8413
Yuanping Yi: 0000-0002-0052-9364
Zhigang Shuai: 0000-0003-3867-2331

Notes

The authors declare no competing financial interest.

■ ACKNOWLEDGMENTS

This work is supported by the National Natural Science Foundation of China (Grant no.21290191 and 91333202). We are grateful to Prof. S. Ramasesha (IISc) for stimulating discussions. Computational resources are supported by Tsinghua National Laboratory for Information Science and Technology.

■ REFERENCES

(1) Shockley, W.; Queisser, H. J. Detailed balance limit of efficiency of p−n junction solar cells. *J. Appl. Phys.* **1961**, *32*, 510−519.

(2) Congreve, D. N.; Lee, J.; Thompson, N. J.; Hontz, E.; Yost, S. R.; Reusswig, P. D.; Bahlke, M. E.; Reineke, S.; Van Voorhis, T.; Baldo, M. A. External quantum efficiency above 100% in a singlet-exciton-fission-based organic photovoltaic cell. *Science* **2013**, *340*, 334−337.

(3) Smith, M. B.; Michl, J. Singlet fission. *Chem. Rev.* **2010**, *110*, 6891−6936.

(4) Smith, M. B.; Michl, J. Recent advances in singlet fission. *Annu. Rev. Phys. Chem.* **2013**, *64*, 361−386.

(5) Busby, E.; Xia, J.; Wu, Q.; Low, J. Z.; Song, R.; Miller, J. R.; Zhu, X.; Campos, L. M.; Sfeir, M. Y. A design strategy for intramolecular singlet fission mediated by charge-transfer states in donor-acceptor organic materials. *Nat. Mater.* **2015**, *14*, 426−433.

(6) Sanders, S. N.; Kumarasamy, E.; Pun, A. B.; Trinh, M. T.; Choi, B.; Xia, J.; Taffet, E. J.; Low, J. Z.; Miller, J. R.; Roy, X.; et al. Quantitative Intramolecular Singlet Fission in Bipentacenes. *J. Am. Chem. Soc.* **2015**, *137*, 8965−8972.

(7) Sanders, S. N.; Kumarasamy, E.; Pun, A. B.; Steigerwald, M. L.; Sfeir, M. Y.; Campos, L. M. Intramolecular Singlet Fission in Oligoacene Heterodimers. *Angew. Chem.* **2016**, *128*, 3434−3438.

(8) Korovina, N. V.; Das, S.; Nett, Z.; Feng, X.; Joy, J.; Haiges, R.; Krylov, A. I.; Bradforth, S. E.; Thompson, M. E. Singlet fission in a covalently linked cofacial alkynyltetracene dimer. *J. Am. Chem. Soc.* **2016**, *138*, 617−627.

(9) Musser, A. J.; Al-Hashimi, M.; Maiuri, M.; Brida, D.; Heeney, M.; Cerullo, G.; Friend, R. H.; Clark, J. Activated singlet exciton fission in a semiconducting polymer. *J. Am. Chem. Soc.* **2013**, *135*, 12747−12754.

(10) Zhai, Y.; Sheng, C.; Vardeny, Z. V. Singlet fission of hot excitons in π-conjugated polymers. *Philos. Trans. R. Soc., A* **2015**, *373*, 20140327.

(11) Kasai, Y.; Tamai, Y.; Ohkita, H.; Benten, H.; Ito, S. Ultrafast Singlet Fission in a Push-Pull Low-Bandgap Polymer Film. *J. Am. Chem. Soc.* **2015**, *137*, 15980−15983.

(12) Zimmerman, P. M.; Zhang, Z.; Musgrave, C. B. Singlet fission in pentacene through multi-exciton quantum states. *Nat. Chem.* **2010**, *2*, 648−652.

(13) Zeng, T.; Hoffmann, R.; Ananth, N. The low-lying electronic states of pentacene and their roles in singlet fission. *J. Am. Chem. Soc.* **2014**, *136*, 5755−5764.

(14) Feng, X.; Luzanov, A. V.; Krylov, A. I. Fission of entangled spins: An electronic structure perspective. *J. Phys. Chem. Lett.* **2013**, *4*, 3845−3852.

(15) Aryanpour, K.; Shukla, A.; Mazumdar, S. Theory of singlet fission in polyenes, acene crystals, and covalently linked acene dimers. *J. Phys. Chem. C* **2015**, *119*, 6966−6979.

(16) Feng, X.; Krylov, A. I. On couplings and excimers: lessons from studies of singlet fission in covalently linked tetracene dimers. *Phys. Chem. Chem. Phys.* **2016**, *18*, 7751−7761.

(17) Feng, X.; Casanova, D.; Krylov, A. I. Intra-and Intermolecular Singlet Fission in Covalently Linked Dimers. *J. Phys. Chem. C* **2016**, *120*, 19070−19077.

(18) Tavan, P.; Schulten, K. Electronic excitations in finite and infinite polyenes. *Phys. Rev. B: Condens. Matter Mater. Phys.* **1987**, *36*, 4337.

(19) Chandross, M.; Shimoi, Y.; Mazumdar, S. Systematic characterization of excited states in conjugated polymers. *Synth. Met.* **1997**, *85*, 1001−1006.

(20) Chien, A. D.; Molina, A. R.; Abeyasinghe, N.; Varnavski, O. P.; Goodson, T., III; Zimmerman, P. M. Structure and Dynamics of the 1 (TT) State in a Quinoidal Bithiophene: Characterizing a Promising Intramolecular Singlet Fission Candidate. *J. Phys. Chem. C* **2015**, *119*, 28258−28268.

(21) Momeni, M. R. Intramolecular Singlet Fission in Quinoidal Bi- and Tetrathiophenes: A Comparative Study of Low-Lying Excited Electronic States and Potential Energy Surfaces. *J. Chem. Theory Comput.* **2016**, *12*, 5067−5075.

(22) Aryanpour, K.; Dutta, T.; Huynh, U. N.; Vardeny, Z. V.; Mazumdar, S. Theory of primary photoexcitations in donor-acceptor copolymers. *Phys. Rev. Lett.* **2015**, *115*, 267401.

DOI: 10.1021/acs.jpclett.7b00656
J. Phys. Chem. Lett. 2017, 8, 2175−2181

(23) Busby, E.; Xia, J.; Low, J. Z.; Wu, Q.; Hoy, J.; Campos, L. M.; Sfeir, M. Y. Fast Singlet Exciton Decay in Push−Pull Molecules Containing Oxidized Thiophenes. *J. Phys. Chem. B* **2015**, *119*, 7644−7650.
(24) Shuai, Z.; Brédas, J. Coupled-cluster approach for studying the electronic and nonlinear optical properties of conjugated molecules. *Phys. Rev. B: Condens. Matter Mater. Phys.* **2000**, *62*, 15452.
(25) White, S. R. Density matrix formulation for quantum renormalization groups. *Phys. Rev. Lett.* **1992**, *69*, 2863.
(26) Shuai, Z.; Bredas, J.-L.; Pati, S. K.; Ramasesha, S. Quantum confinement effects on the ordering of the lowest-lying excited states in conjugated polymers. *Proc. SPIE* **1997**, *3145*, 293−302.
(27) Chan, G. K.-L.; Sharma, S. The density matrix renormalization group in quantum chemistry. *Annu. Rev. Phys. Chem.* **2011**, *62*, 465−481.
(28) Ren, J.; Yi, Y.; Shuai, Z. Inner space perturbation theory in matrix product states: Replacing expensive iterative diagonalization. *J. Chem. Theory Comput.* **2016**, *12*, 4871−4878.
(29) Ramasesha, S.; Pati, S. K.; Krishnamurthy, H.; Shuai, Z.; Brédas, J. Symmetrized density-matrix renormalization-group method for excited states of Hubbard models. *Phys. Rev. B: Condens. Matter Mater. Phys.* **1996**, *54*, 7598.
(30) Pople, J. Electron interaction in unsaturated hydrocarbons. *Trans. Faraday Soc.* **1953**, *49*, 1375−1385.
(31) Pariser, R.; Parr, R. G. A Semi-Empirical Theory of the Electronic Spectra and Electronic Structure of Complex Unsaturated Molecules. I. *J. Chem. Phys.* **1953**, *21*, 466−471.
(32) Frisch, M. J.; Trucks, G. W.; Schlegel, H. B.; Scuseria, G. E.; Robb, M. A.; Cheeseman, J. R.; Scalmani, G.; Barone, V.; Mennucci, B.; Petersson, G. A. et al. *Gaussian09*, revision D.01; Gaussian, Inc.: Wallingford, CT, 2009.
(33) Oliva, M. M.; Casado, J.; Navarrete, J. T. L.; Patchkovskii, S.; Goodson, T., III; Harpham, M. R.; Seixas de Melo, J. S.; Amir, E.; Rozen, S. Do [all]-S, S-Dioxide Oligothiophenes Show Electronic and Optical Properties of Oligoenes and/or of Oligothiophenes? *J. Am. Chem. Soc.* **2010**, *132*, 6231−6242.
(34) Zerner, M.; Ridley, J.; Bacon, A.; Edwards, W.; Head, J.; McKelvey, J.; Culberson, J.; Knappe, P.; Cory, M.; Weiner, B. et al. *ZINDO: A semi-empirical program package*; University of Florida: Gainesville, FL, 1999.
(35) Martin, R. L. Natural transition orbitals. *J. Chem. Phys.* **2003**, *118*, 4775−4777.
(36) Kolomeisky, A. B.; Feng, X.; Krylov, A. I. A simple kinetic model for singlet fission: A role of electronic and entropic contributions to macroscopic rates. *J. Phys. Chem. C* **2014**, *118*, 5188−5195.
(37) Barford, W. *Electronic and optical properties of conjugated polymers*; Oxford University Press: Oxford, U.K., 2013.
(38) Barford, W.; Bursill, R. J.; Lavrentiev, M. Y. Density-matrix renormalization-group calculations of excited states of linear polyenes. *Phys. Rev. B: Condens. Matter Mater. Phys.* **2001**, *63*, 195108.
(39) Luzanov, A. V.; Casanova, D.; Feng, X.; Krylov, A. I. Quantifying charge resonance and multiexciton character in coupled chromophores by charge and spin cumulant analysis. *J. Chem. Phys.* **2015**, *142*, 224104.
(40) Clark, A. E.; Davidson, E. R. Local spin. *J. Chem. Phys.* **2001**, *115*, 7382−7392.
(41) Matsika, S.; Feng, X.; Luzanov, A. V.; Krylov, A. I. What We Can Learn from the Norms of One-Particle Density Matrices, and What We Can't: Some Results for Interstate Properties in Model Singlet Fission Systems. *J. Phys. Chem. A* **2014**, *118*, 11943−11955.
(42) Hu, W.; Chan, G. K.-L. Excited-State Geometry Optimization with the Density Matrix Renormalization Group, as Applied to Polyenes. *J. Chem. Theory Comput.* **2015**, *11*, 3000−3009.
(43) Englman, R.; Jortner, J. The energy gap law for radiationless transitions in large molecules. *Mol. Phys.* **1970**, *18*, 145−164.

DOI: 10.1021/acs.jpclett.7b00656
J. Phys. Chem. Lett. 2017, 8, 2175−2181